Spectral characteristics of a relativistic plasma microwave generator

M. V. Kuzelev, O. T. Loza, A. V. Ponomarev, A. A. Rukhadze, P. S. Strelkov, D. K. Ul'yanov, and A. G. Shkvarunets

Institute of General Physics, Russian Academy of Sciences, 117942 Moscow, Russia
(Submitted 7 December 1995)
Zh. Éksp. Teor. Fiz. **109**, 2048–2063 (June 1996)

The radiation spectrum of a broad-band relativistic plasma microwave generator, in which a hollow relativistic electron beam is injected into a plasma waveguide consisting of a hollow plasma within a round metallic waveguide is measured experimentally. The radiation spectrum is measured using a wide-aperture calorimetric spectrometer in the frequency range 3–32 GHz. The influence of the plasma density and the beam–plasma gap on the radiation spectrum is investigated. The amplification of the noise electromagnetic radiation when a relativistic electron beam is injected into the plasma waveguide is calculated on the basis of the nonlinear theory. The theory predicts passage from a one-particle generation regime to a collective regime and narrowing of the radiation spectrum as the plasma density and the gap between the hollow beam and the plasma increases. A comparison of the measurement results with the nonlinear theory accounts for several features of the measured spectrum. However, the predicted change in the generation regimes is not observed experimentally. Qualitative arguments are advanced, which explain the observed phenomena and call for further theoretical and experimental research, are advanced. [S1063-7761(96)01006-2]

1. INTRODUCTION

Plasma microwave electronics appeared after the 1949 papers by A. I. Akhiezer and Ya. B. Faĭnberg[1] and by D. Bohm and E. P. Gross,[2] who discovered the phenomenon of beam–plasma instability and predicted the efficient excitation of microwaves in a plasma by dense electron beams. These papers stimulated the performance of numerous theoretical and experimental studies throughout the world. However, experimental plasma microwave electronics remained nonrelativistic until the end of the seventies, since nonrelativistic electron beams were used in the experiments. This was responsible for many problems, which have been overcome with varying degrees of success. All this was excellently described in the first monographs[3,4] and in a relatively recent review.[5]

Relativistic plasma microwave electronics began to be developed at the end of the seventies. It was given a great boost by the first successful experiment[6] creating an effective relativistic plasma microwave generator in 1982. At approximately the same time theoreticians conclusively established that beam–plasma instability is the stimulated Cherenkov emission of dense electron beams in a plasma and that the relativistic character of the electron energy should significantly increase the emissivity of the plasma. The principles of the theory of the stimulated Cherenkov emission of dense relativistic electron beams in a plasma and of relativistic plasma microwave electronics were formulated in papers published in the eighties, and they have been elaborated in reviews (Refs. 7 and 8), books of collected works (Refs. 9 and 10), and a monograph (Ref. 11).[1)]

After the general principles of the theory were established, systematic experimental studies were undertaken in close contact with the theory, which endeavored to take into account the specific features of the experiments. The results of the first experiments, which were summarized in the review in Ref. 12, confirmed the main conclusions of the theory: the existence of a threshold value of the plasma density, above which the generation of microwave radiation appeared in the system, the presence of a minimum current (or a minimum length of the interaction system), and a fairly high radiation efficiency $\approx 20\%$. The generation frequency was measured very roughly in the first experiments, but it increased with increasing plasma density as long as the radiation efficiency remained high; at high densities the radiation efficiency decreases in accordance with the theoretical predictions. The experimental data were in qualitatively good agreement with the conceptions regarding the excitation of the axially symmetric TM-mode (cable wave) of a metallic waveguide filled by a hollow plasma. The main radiated power of this wave is concentrated in the gap between the hollow plasma and the metallic waveguide.

The results of more detailed investigations of the dependences of the radiated power on the plasma density, the relativistic beam current, and the length of the interaction system were summarized in the review in Ref. 13. The measured azimuthal distribution of the power was consistent with the hypothesis that the axially symmetric ($l=0$) mode of the plasma cable wave is excited. This made it possible to calculate the nonlinear dependence of the radiated power on the beam current. A comparison of the calculated dependence with experiment confirmed that a one-particle, or Compton, mechanism of stimulated Cherenkov emission operated in the microwave generator. The measured dependence of the radiated power on the plasma density and the cavity length also agreed well with the theory. However, the most important experimental results were the high radiation efficiency ($\sim 20\%$) and the absolute value of the radiated power, which exceeded 300 MW. These achievements placed relativistic plasma microwave electronics on the level of vacuum rela-

 1063-7761/96/061102-10$10.00

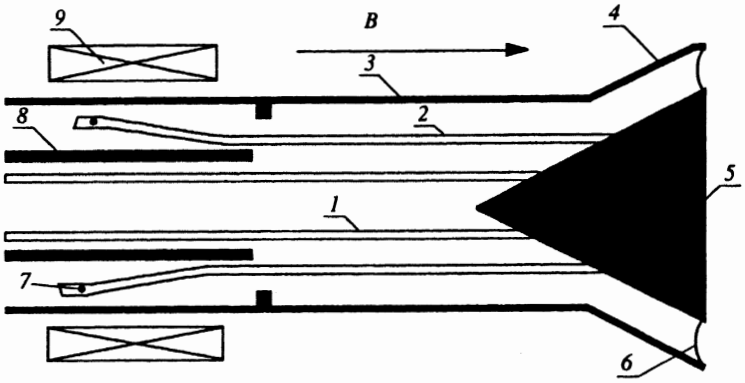

FIG. 1. Schematic representation of a plasma microwave generator: *1* — electron beam, *2* — plasma, *3* — metallic waveguide, *4* — coaxial conical radiating horn, *5* — collector, *6* — dielectric window, *7* — hot annular cathode of the plasma source, *8* — copper tube, *9* — coil of the "fast" magnetic field.

tivistic microwave electronics and attested to its competitiveness.

The experimental results described in Refs. 12 and 13, however, had two significant deficiencies. First, there were practically no measurements of the radiation spectra in them. Second, the absolute measurements of the total radiated energy and power exhibited poor precision. During the last few years the main efforts of experimentalists were aimed at overcoming these deficiencies. A sensitive calorimeter, which receives the radiation from the entire aperture of the emitter and measures the energy with an accuracy of ~ 0.05 J, was constructed.[14]

The first attempt to measure a spectrum was undertaken in our laboratory.[14,15] However, the range of the spectrum analyzer, 8–17 GHz, was narrower than the spectrum of the plasma microwave generator. In addition, the radiation was measured at several points in this range in relative units. Therefore, the experimental and theoretical results could not be compared quantitatively. The main conclusions regarding the qualitative agreement with the linear theory, the broadband character of the radiation, and the possibility of tuning the mean frequency were of great interest.

Therefore, we developed a new spectrometer, which has a broader frequency range (3–32 GHz) and makes it possible to measure the absolute value of the energy of the complete radiation flux in the assigned frequency subranges, into which the entire range was divided.

The purpose of the present investigation is to experimentally study the dependence of the radiation spectrum on the plasma density and the size of the gap between the hollow beam and the plasma and to compare it with the results of a calculation of the amplification bands on the basis of the linear theory and a nonlinear calculation of the spectrum. As will be shown below, the theory predicts passage from a Compton generation mechanism (when the gap is small and the plasma density is relatively low) to a Raman mechanism (when the gap is large and the plasma density is high). The change in mechanism is manifested by a change in the character of the spectrum. In our opinion, this phenomenon is of great physical interest.

2. EXPERIMENTAL MEASUREMENTS AND RESULTS

1. Experimental setup

The main component of the apparatus is the Terek-2 accelerator. The parameters of the relativistic electron beam (REB) were fixed: energy, 540 keV; current, 2.4 kA; current pulse duration, 30 ns. A schematic representation of the experiment is shown in Fig. 1. The hollow electron beam *1* with a thickness $\Delta_b \approx 1$ mm passes within the hollow cylindrical plasma *2* with a thickness $\Delta_p \approx 1$ mm. The coaxial plasma waveguide consisting of the hollow plasma and the metallic waveguide *3* passes into the coaxial conical horn, in which the external (*4*) and the internal (*5*) cones are metallic. The radiation is generated in the plasma waveguide. It then enters the metallic coaxial conical horn and is emitted into the atmosphere through the dielectric window *6*.

It was previously noted[16] that the microwave radiation efficiency depends strongly on the gap between the hollow plasma and the beam. The theory in Ref. 11 also predicts the possibility of considerable variation of the radiation parameters and, as has already been mentioned in the introduction, even a change in the instability mechanism in response to a comparatively small change in the gap between the beam and the plasma. In our experiments the beam radius was fixed ($R_b = 0.65$ cm), and the plasma radius was varied ($R_p = 0.8$–1.1 cm). The possibility of varying the plasma radius from shot to shot represents the most significant design difference between the present and preceding experimental setups.

The electron beam and the plasma were immersed in a longitudinal uniform steady magnetic field $B_0 = 17$ kG with a half-period $T/2 = 3.5$ ms. As previously,[12,13] the plasma was created in a discharge with a hot annular cathode (*7* in Fig. 1). The parameters of the plasma source were as follows: voltage on the cathode, 600 V, discharge current, 5–150 A; pressure in the chamber, $P = 10^{-3}$ torr; gas, xenon. The coil *9* of the fast magnetic field, which made it possible to reduce the magnetic field on the hot cathode of the plasma source to zero, was located in the vicinity of the hot cathode. The half-period of the fast field was 100 μs. The copper tube *8* was inserted into the hot annular cathode. The thickness and width of the tube were selected so that switching on the magnetic field of the fast coil would not distort the magnetic field on the axis of the system (the weakening of the field on the axis was $\leqslant 10\%$). As a result, for a time of order 20 μs the hot cathode is in a constant, low-strength magnetic field, and the relativistic beam is then in a uniform (to within 10%) magnetic field over the entire distance from the cathode to the collector. This level of uniformity precludes "pumping" of the transverse velocity of the relativistic electrons, which

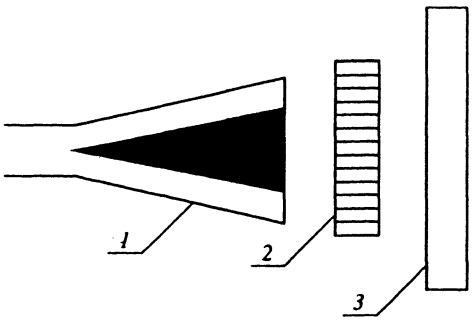

FIG. 2. Spectrometer: *1* — radiating horn, *2* — low-frequency filter, *3* — calorimeter.

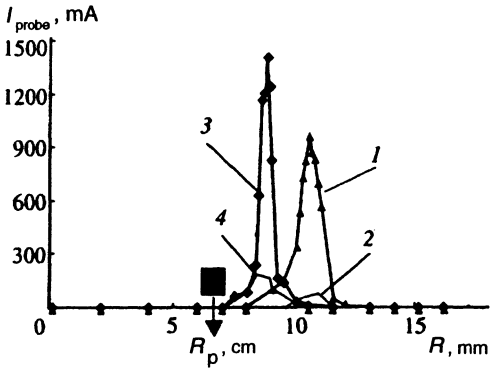

FIG. 3. Dependence of the electron current onto the probe on the radius: *1* and *2* — fast coil switched off (*1* — $U_{probe}=+15$ V, *2* — $U_{probe}=-15$ V); *3* and *4* — fast coil switched on (*3* — $U_{probe}=+15$ V, *4* — $U_{probe}=-15$ V). The radius of the relativistic beam R_b is plotted in the figure, and its thickness ΔR_b is indicated by the hatching.

is very important for achieving highly efficient stimulated Cherenkov emission. The fast coil weakens the magnetic field in a region which is small in comparison with the length of the plasma in the vicinity of the plasma source cathode, where the beam is prevented from interacting with the plasma by the copper tube. It is easy to understand that variation of the strength of the magnetic field of the fast coil makes it possible to regulate the diameter of the plasma in the waveguide from shot to shot in the range from the diameter of the hot cathode to the diameter of the copper tube, while the diameter of the relativistic electron beam remains unchanged. Supplying current to the fast coil in the opposite direction provides for regulation of a plasma diameter exceeding the diameter of the plasma source cathode.

2. Diagnostics

The value of the current in the plasma source, which, according to preliminary measurements, corresponds to a definite value of the plasma density, was recorded as the relativistic electron beam passed through the plasma. The voltage on the accelerator cathode, the strengths of the principal magnetic field and the field of the fast coil, the pressure of the gas, and the parameters of the microwave radiation were recorded in each shot. The radiated microwave power was measured by a traditional semiconductor "hot electron" detector and the new wide-aperture calorimeter. The detector was used to investigate the time dependence of the power density of the microwave radiation, which, together with the measurements of the total radiated energy using the calorimeter, made it possible to calculate the absolute value of the radiated power.

The most important results were obtained using the calorimetric spectrometer, which is schematically represented in Fig. 2. The radiation from the coaxial horn enters the low-frequency field and then the calorimeter. There was a set of filters (five), which transmit the frequencies $f>f_n$, $n=1,2,\ldots 5$, where $f_1=6$ GHz, $f_2=9$ GHz, $f_3=15.3$ GHz, $f_4=24.3$ GHz, $f_5=32.3$ GHz. For $f<f_n$, the filters are completely opaque, and for $f>f_n$ the filters have different transparencies, which vary in the range from 61% to 78% for the different filters and do not depend on the polarization of the radiation. The spectrum was measured in the following manner. The radiated energy was first recorded without a filter. Then the five filters were inserted in turn, and the energy passing through each of them was measured. The radiated energy in each particular frequency band can be determined by subtracting the readings of the calorimeter in two successive measurements.

The accuracy of the measurement of the spectrum by this method depends, first of all, on the stability of the spectrum from shot to shot. To obtain reliable information, it was necessary to average the readings of the calorimeter with a specific filter for five shots. Both the statistical errors and the error of the calorimetric measurements were taken into account on the experimental plot.

One deficiency of this method, which is associated with the statistics, will hopefully be eliminated in the future. Another deficiency, which is associated with the lack of temporal resolution, cannot be eliminated in principle.

On the other hand, one tremendous advantage of the method is the high reliability of the measurement of the absolute values of the total radiated energy in a given frequency band. We note that in relativistic microwave electronics the radiation detector generally picks up a small part of the complete radiation flux from the microwave generator and can, in principle, record different spectra at different points in the radiation field. Measuring the spectrum of the complete radiation flux greatly facilitates the possibility of comparing theory with experiment.

3. Experimental results

As we have already noted in the introduction, the main purpose of the present work was to measure the spectral characteristics of microwave radiation as a function of the plasma density with different gaps between the plasma and the beam. Therefore, we shall dwell first on the results of the measurements of the plasma characteristics.

a) Measurement of the plasma characteristics

The radial profile of the plasma density was measured by a single annealed probe. The diameter of the probe was 0.2 mm, and it was displaced with a spacing of 0.25 mm. Figure 3 shows profiles of the current density onto the probe when the probe potential equals +15 V (curves *1* and *3*) and

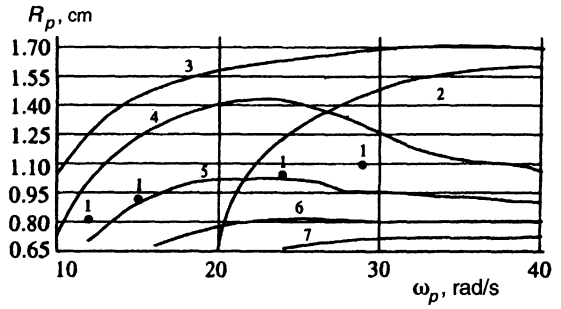

FIG. 4. Threshold plasma density for the appearance of microwave generation for various radii of the hollow plasma (R_b=const=0.65 cm): *1* — experimental points of the threshold values of the plasma density for various values of R_p; *2* — theoretical dependence of the threshold value of the Langmuir frequency $\omega_p(R_p)$ for the case of $\omega_b=0$; *3*, *4*, *5*, *6*, *7*, – calculated curves on which the constant values $\delta k=0.0$, 0.1, 0.2, 0.3, and 0.4, respectively, are achieved under the conditions $\gamma=2$, $I_b=2$ kA, $R_b=0.65$ cm, $\Delta_p=\Delta_b=0.1$ cm, $R=1.8$ cm.

-15 V (curves *2* and *4*), curves *3* and *4* corresponding to the fast coil switched on and curves *1* and *2* corresponding to this coil switched off.

The electrical current onto the probe when the potential is $+15$ V is determined by the saturation electron current of the low-temperature ($\sim$3 eV) plasma and the discharge current of the plasma source. When the discharge current equals 80 A, the current onto the collector equals $\sim$30 A. It follows from the ratio between the cross section of the plasma ($\sim$60 mm^2) and the area of the probe ($\sim$0.3 mm^2) that a part of the total current onto the collector equal to $\sim$0.15 A should impinge on the probe, as is observed in an approximation when the potential equals -15 V. Since the current drawn by the probe that is associated with the presence of the discharge current of the plasma source is small compared with the current of thermal electrons and since the drift velocity of the electrons is relatively high ($\mathcal{E}_e>15$ eV), it can be stated that the plasma density profile is determined approximately by curves *1* and *3* in Fig. 3. Hence it follows that the characteristic thickness of the hollow plasma is $\sim$1 mm, which corresponds to a diameter of the tungsten cathode wire equal to 0.8 mm. It is also seen that switching on the magnetic field of the fast coil in this experiment reduces the plasma diameter from 21 mm to 17 mm.

The absolute value of the plasma density was measured by the cavity microwave method. Each value of the discharge current (for fixed values of the magnetic field and the gas pressure) corresponds to a definite value of the plasma density.

b) Measurement of the threshold plasma density

The threshold value of the plasma density was determined from plots of the dependence of the radiated microwave power on the plasma density by extrapolating these curves to a zero value for the power. The threshold values of the plasma frequency ω_p determined in this manner for a fixed beam radius $R_b=0.65$ cm and a fixed beam current $I_b=2$ kA are represented by the circles in Fig. 4 for different radii R_p of the hollow plasma from 0.8 cm to 1.1 cm. These values differed significantly from the theoretical predictions for the small beam current at which the threshold values are determined by curve *2*. An explanation for this disparity can be obtained by taking into account the beam current and is given in Sec. 3.

c) Measurement of the microwave radiation spectrum

The main result of the measurement of the microwave radiation spectrum is presented in Fig. 5. It is noteworthy that the shapes of the microwave signals recorded by the semiconductor detector are approximately the same both in the absence of filters and when the radiation which has passed through various filters is detected. The signal has a bell-shaped form with a half-width of 18 ns. This means that the entire spectrum is emitted simultaneously by the generator. Each plot in Fig. 5 represents the result of the averaging of 30 shots. Accordingly, the mean value of the radiated energy in each particular series of shots is plotted on each graph. The maximum energy in a pulse reached 1.5 J, which corresponds to a maximum radiated power equal to 85 MW and a radiation efficiency equal to 7%. We note that an efficiency of $\approx$20% was recorded in the preceding study.[14] This difference is apparently attributable to the different beam current pulse durations: $\sim$ 30 ns in the present work and $\sim$100 ns in Ref. 14. This hypothesis is confirmed by the shape of the microwave signals in Ref. 14, which reached a maximum at $\sim$50 ns. It should also be added that in the theory of a stationary accelerator the efficiency is equal to $\approx$20% for our beam, plasma, and waveguide parameters. As previously,[14] the maximum radiated energy is observed near the threshold plasma density and slightly above it, and then the radiated energy decreases as the plasma density increases. It is seen from Fig. 5 that when the threshold plasma density is exceeded by a factor of 8, the radiated intensity decreases by a factor of 2.

The spectra for $R_p=0.8$ cm and three values of the plasma density, viz., $n_p=1.5\times10^{13}$ cm^{-3}, 3×10^{13} cm^{-3}, and 3.8×10^{13} cm^{-3}, are presented on the left-hand side of Fig. 5. All three spectra have two maxima, one in the low-frequency region and the other in the high-frequency region. Both maxima shift toward higher frequencies as the plasma density increases: the low-frequency maximum shifts from 0–6 GHz to 9–15 GHz, and the high-frequency maximum shifts from 15–32 GHz to 24–32 GHz.

Increasing the plasma diameter to 21 mm when $n_p=3\times10^{13}$ cm^{-3} does not qualitatively alter the spectrum. When the plasma density equals 3.8×10^{13} cm^{-3} and the diameter equals 21 mm, merging of the two maxima is observed, and broad-band radiation, which is uniform over the entire range from 9 to 32 GHz, is recorded.

It was noted in our preceding communication[14] that the shift of the generation band toward higher frequencies as the plasma density increases is consistent with linear theory, specifically with the frequency dependence of the gain coefficient on the plasma density. The generation discovered in two frequency ranges, the presence of the low-frequency part of the radiation, and especially the broad-band character of the spectrum at high plasma densities stimulated further de-

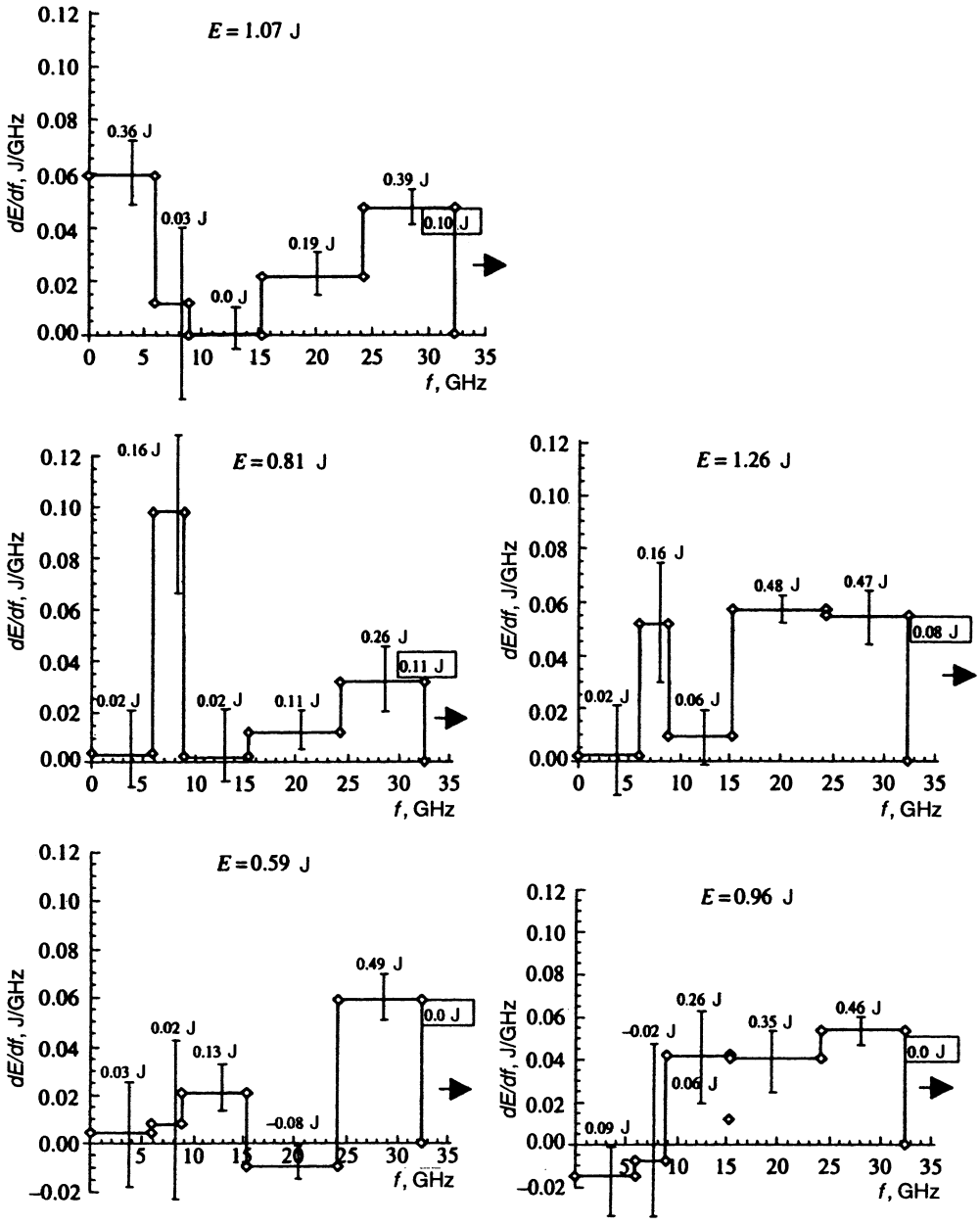

FIG. 5. Experimental spectra. The left-hand spectra were measured with a plasma radius $R_p=0.8$, cm and the right-hand spectra were measured with $R_p=1.05$ cm. The uppermost spectrum was measured with $n_p=1.5\times10^{13}$ cm^{-3} ($f_p=34$ GHz), those in the middle row were measured with $n_p=3\times10^{13}$ cm^{-3} ($f_p=48$ GHz), and those in the lower row were measured with $n_p=3.8\times10^{13}$ cm^{-3} ($f_p=54$ GHz). The threshold value of the plasma density for $R_p=0.8$ cm equals 5×10^{12} cm^{-3}, and the value for $R_p=1.05$ cm equals 2×10^{13} cm^{-3}.

velopment of the theoretical ideas, which are discussed in the next section.

3. RESULTS OF THE THEORETICAL ANALYSIS AND COMPARISON WITH EXPERIMENT

The general theory for a relativistic plasma microwave generator with an arbitrary profile of the plasma density in the waveguide has been presented in a monograph.[11] Here, we present only the results that are applicable to the specific experiment described above.

1. Linear theory, kinetic approximation

We present some results of the linear theory pertaining to calculations of the dispersion characteristics of a plasma waveguide and the thresholds for the excitation of electromagnetic waves associated with the stimulated Cherenkov interaction of a monoenergetic thin hollow beam with a hollow plasma in the approximation of an infinitesimal current, which is known as the kinematic approximation.

Figure 6 presents the dispersion curve for the azimuthally symmetric ($l=0$) mode of the surface wave (curve *1*) of a thin-walled hollow plasma for a mean radius $R_p=1$ cm, a thickness $\Delta_p=0.1$ cm, a radius of the metallic waveguide

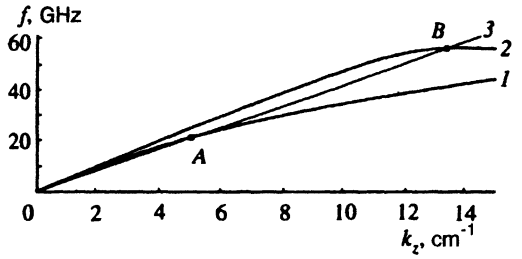

FIG. 6. Dispersion curves of waves in a round plasma-filled waveguide: *1* — hollow plasma with $R_p<R$ and an infinitesimal thickness $\Delta_p\to 0$, *2* — uniform filling of the waveguide by the plasma, *3* — the straight line $\omega=k_z u$. *A* and *B* — particle–wave resonance points.

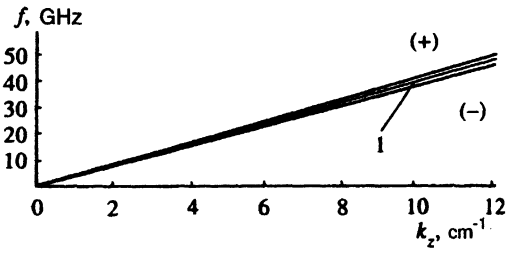

FIG. 7. Dispersion curves of the electron beam: $I_b=2$ kA, $u=2.6\times 10^{10}$ cm/s, $R_b=0.65$ cm, $\Delta_b=0.1$ cm, $R=1.8$ cm; curve *1* corresponds to $\omega=k_z u$.

$R=1.8$ cm, and a plasma frequency $f_p=56$ GHz (i.e., $n_p=4\times 10^{13}$ cm^{-3}). The initial linear portion of this curve corresponds to the familiar plasma cable wave.[11] Curve *2* in the same figure depicts the fundamental ($n=1$) azimuthally symmetric ($l=0$) mode of an internal wave in a waveguide completely filled with a homogeneous plasma. It is seen that this curve is considerably steeper and abruptly reaches a plateau at the plasma frequency where the wave becomes electrostatic. Here curve *3* is the straight line $\omega=k_z u$, which defines the dispersion law of a beam wave at a vanishingly small beam density. In this case $u=2.6\times 10^{10}$ cm/s, which corresponds to $\gamma=2$. Point *A* corresponds to resonance of the beam with the surface wave, and point *B* corresponds to resonance with the internal wave. It is seen that resonance with the surface wave occurs on the linear portion of the dispersion curve, where the wave is strongly electromagnetic and is readily emitted from the plasma (since $u\approx c$), while point *B*, which corresponds to resonance of the beam with the internal wave, is located on the portion of the curve defined by the relation $\omega\sim\omega_p$, where the wave is almost electrostatic and therefore not emitted from the plasma.

Thus, the differences in the plasma-density profiles have a strong effect on the dispersion law and the condition for Cherenkov resonance. It is seen from Fig. 6, that the group velocity of the wave is significantly greater in case *A* than in case *B*. This circumstance was one of the reasons for selecting the type of plasma coaxial waveguide with a hollow plasma of small thickness. Stimulated Cherenkov emission with a higher efficiency should naturally be expected in such a geometry, especially when the current in the relativistic electron beam is large. It should be noted in passing that the resonance point *A* corresponds to a radiation frequency of $\approx$20 GHz, i..e, which is considerably below $f_p=56$ GHz, in agreement with the experiment described above.

We note another advantage of the use of a plasma coaxial waveguide. In the region of the collector the coaxial plasma waveguide passes into a smoothly expanding conical metallic coaxial waveguide. The structures of the fields in both waveguides practically coincide for $\omega\ll\omega_p$ (point *A* lies just in this region) and $u\approx c$; therefore, for the reflectivity from the region of the transition from one waveguide to the other we can use the approximate formula

$$k\approx\frac{1}{4\gamma^2}, \tag{3.1}$$

which points out the high transparency of the region of the transition from one coaxial waveguide to the other for $\gamma=2$ and the low Q factor of the plasma microwave cavity, which is a very important characteristic of high-current high-power microwave systems.

Finally, let us discuss the question of the threshold values of the plasma density in the limit of an infinitesimal beam current. These values are obtained by substituting the condition $\omega=k_z u$ into the dispersion relations of a plasma waveguide. As a result, for the value of the threshold plasma density at which Cherenkov emission appears we have[11]

$$\omega_p^*=k_{\perp\min}\,u\gamma, \tag{3.2}$$

where in the case of complete filling of the waveguide by the plasma $k_{\perp\min}$ corresponds to excitation of the fundamental symmetric mode of vibration with

$$k_{\perp\min}=2.4/R. \tag{3.3}$$

For $R=1.8$ cm and $u=2.6\times 10^{10}$ cm/s we obtain $\omega_p^*=7\times 10^{10}$ s^{-1} or $n_p^*=1.6\times 10^{12}$ cm^{-3}.

If the plasma waveguide has the form of a coaxial structure with a thin hollow plasma of radius R_p and thickness Δ_p, we have

$$k_{\perp\min}=(R_p\Delta_p\ln(R/R_p))^{-1/2}. \tag{3.4}$$

When $R_p=1$ cm, $\Delta_p=0.1$ cm, and $R=1.8$ cm, for a beam with $u=2.6\cdot 10^{10}$ cm/s we find $\omega_p^*=2.1\times 10^{11}$ s^{-1} or $n_p^*=1.5\times 10^{13}$ cm^{-3}.

2. Linear theory with consideration of the finite value of the beam current

Moving on to the question of the excitation of a plasma microwave generator by a relativistic electron beam, we first of all consider the intrinsic waves of the thin-walled hollow beam in a waveguide in the absence of a plasma, but with consideration of a finite beam density. The dispersion law of beam waves is presented in Fig. 7. The dispersion curves were constructed for the specific relativistic electron beam parameters indicated above: $I_b=2$ kA, $u=2.6\times 10^{10}$ cm/s, $R_b=0.65$ cm, $\Delta_b=0.1$ cm, and $R=1.8$ cm. We note that a wave with a high phase velocity is called a fast beam wave and that a wave with a small phase velocity is called a slow beam space-charge wave.

Both an electron beam and a plasma are oscillating systems, and when they are simultaneously present in a wave-

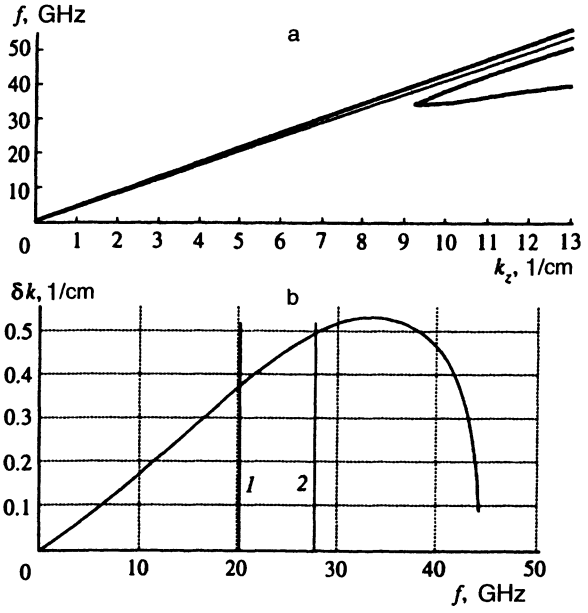

FIG. 8. Compton amplification regime. a — Dispersion curves of waves in a waveguide with a thin-wall hollow beam and a thin-wall hollow plasma when the mean radii of the beam and the plasma coincide. b — Dependence of the gain coefficient δk on the generation frequency f: *1* — particle–wave resonance, *2* — wave–wave resonance. Conditions: $\gamma=2$, $I_b=2$ kA, $R_b=R_p=0.65$ cm, $R=1.8$ cm, $f_p=56$ GHz.

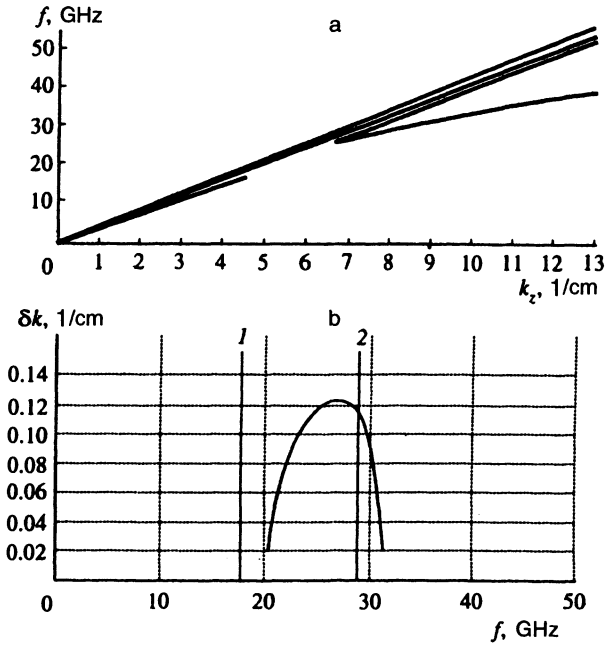

FIG. 9. Raman amplification regime. a — Dispersion curves of waves in a waveguide with a hollow beam and a hollow plasma when the mean radii of the beam and the plasma do not coincide, b — dependence of the gain coefficient δk on the generation frequency f: *1* — particle–wave resonance, *2* — wave–wave resonance. Conditions: $\gamma=2$, $I_b=2$ kA, $R_p=1.1$ cm, $R_b=0.65$ cm, $R=1.8$ cm, $f_p=56$ GHz.

guide, these two oscillating subsystems interact. Having excess energy, the beam subsystem will impart part of its energy to the plasma subsystem as a consequence of stimulated Cherenkov emission, or, stated differently, plasma oscillations will be excited. It is easy to understand that the character of this interaction depends strongly on the relative arrangement of these subsystems. If the subsystems are spatially juxtaposed, the interaction will be strong; as is said in electronics, there is strong coupling between the oscillating subsystems, and the induced emission has a one-particle or Compton character. Conversely, in the case of spatially separated subsystems the coupling weakens, and the emission process goes from a Compton regime to a Raman or collective regime. Of course, the change in the emission regime depends not only on the transverse geometry of the systems, but also on the plasma and beam densities. More specifically, when the plasma and beam densities are high, the transition to a Raman generation regime is clearly facilitated.

The dispersion equation for a plasma–beam system was solved for the case of a thin-walled hollow plasma and thin-walled hollow beam as an amplifier problem. The frequency range in which the gain coefficient $\delta k \equiv \mathrm{Im} k_z(\omega) > 0$, i.e., amplification of the microwave radiation takes place, was determined. We note that the dispersion relations $\omega(k_z)$ were found by solving the exact equations, while δk was found by solving approximate equations. The calculation of δk was performed in the same approximation[2)] as the calculation of the nonlinear spectra described below to permit comparison of their results. Therefore, the amplification bands in Figs. 8a and b, as well as in Figs. 9a and b, differ somewhat.

In the case of a Compton regime, the gain coefficient is high, and amplification takes place over a broad range of frequencies. The dispersion curves $\omega(k_z)$ for the case of equal beam and plasma radii and the real system parameters indicated above ($I_b=2$ kA, $\gamma=2$, $R_b=R_p=0.65$ cm, $\Delta_b=\Delta_p=0.1$ cm, and $R=1.8$ cm) are presented in Fig. 8a. In this case we have a pure Compton amplification regime, the amplification band extends from 0 to 34 GHz (to the turning point of the lower curve, which corresponds to a slow beam wave). This is also seen from Fig. 8b, which shows the frequency dependence of the gain coefficient δk. Vertical straight lines *1* and *2* in this figure correspond to the resonance frequency of the plasma wave and the beam wave $\omega=k_z u$ (particle–wave resonance) and the resonance frequency of the plasma wave and the slow beam wave, which is shown in Fig. 7 (wave–wave resonance). Amplification is observed both at resonances and in regions far from them. The resonances, like δk, were calculated using approximate formulas.

The situation is different in the case in which the radii of the beam and the plasma are not equal, since such a difference leads to a decrease in the gain coefficient and the appearance of a Raman amplification regime. Figure 9 presents the dispersion curves and the gain coefficient for the same beam parameters as in Fig. 8, but for a mean plasma radius greater than the beam radius: $R_p=1.1$ cm, $R_b=0.65$ cm. Such apparently slight separation of the plasma from the beam (the gap between the plasma layer and the beam equals only 3.5 mm) strongly weakens the coupling between them and significantly alters the amplification regime. The amplification band becomes narrow, the gain coefficient peak being close to the wave–wave resonance frequency. In addi-

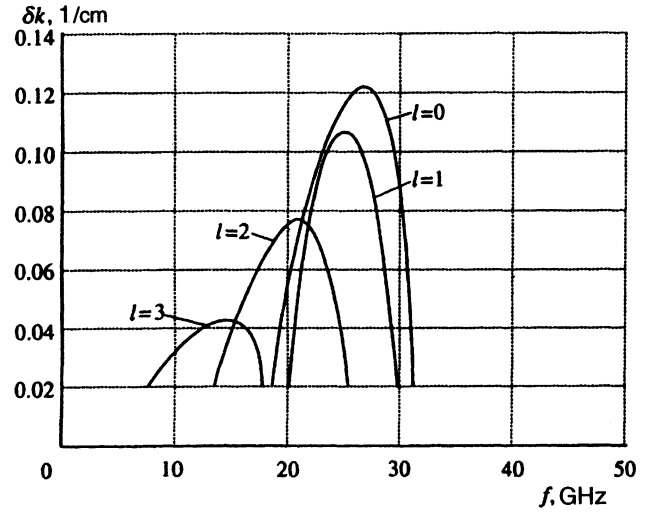

FIG. 10. Frequency dependence of the gain coefficient of the $l=0$ mode and the azimuthally asymmetric modes with $l=1$, $l=2$, and $l=3$. The calculation conditions are the same as in Fig. 9.

tion, there is no amplification at all at the particle–wave resonance frequency.

A large current in a relativistic electron beam can excite asymmetric modes ($l \neq 0$) of the cable wave in a coaxial plasma waveguide. In the theory for a small current in a relativistic electron beam the threshold densities for exciting such modes are higher and the gain coefficient is much smaller than for a symmetric mode. However, when the current increases, these parameters converge, as is clearly seen from Fig. 10, which presents the frequency dependence of the gain coefficients for the modes with $l=0$, 1, 2, and 3 under a Raman regime (the parameters in Fig. 10 correspond to the parameters in Fig. 9). It is seen from Fig. 10 that the $l=1$ mode can, in principle, compete with the $l=0$ mode and that the modes with $l=2$ and 3 have much smaller gain coefficients.

As for the value of the threshold plasma density above which amplification is possible in the system, it is lower than that determined from Eqs. (3.2) and (3.4) when the current in the relativistic electron beam is large. This follows from the fact that the dispersion curve of the slow beam wave lies below the linear plot of $\omega=k_z u$ as the current increases. In Fig. 4 curve *2* corresponds to Eq. (3.2), i.e., it specifies the threshold value of ω_p as a function of R_p for zero relativistic electron beam current. As the beam current increases and a nonzero gain coefficient δk appears, waves can be excited at smaller plasma densities. Figure 4 presents calculated plots of $\delta k=\text{const}$ in the ω_p, R_p plane for the beam parameters indicated above. It is seen that the experimental values of the threshold densities for different plasma radii agree most closely with curve *5*, on which $\delta k=0.2\ \text{cm}^{-1}$.

3. Nonlinear effects and their influence on the radiation spectrum

Figure 11 presents the radiation spectra calculated using the nonlinear theory of a plasma microwave accelerator, whose basic assumptions were described in Ref. 11. The calculation was performed according to the following scheme. Broad-band (much broader than the detection band) white noise of equal intensity throughout the spectrum was fed into the system, and the steady-state radiation spectrum was determined by numerically solving the nonlinear equations for the wave amplitudes. The steady-state spectrum turned out to depend only weakly on the intensity and width of the spectrum of the signal fed into the system.

Figure 11 presents calculated spectra of the accelerator at the point in space where the experimentally observed level of power is achieved. In addition, Fig. 11 presents the experimental spectra of Fig. 5. The linear segment at the top of each graph shows the frequency range in which the gain coefficient δk falls within the range from $0.5dk_{\max}$ to $\delta k_{\max}$ according to the linear theory. The nonlinear theory, of course, gives better agreement with experiment than does the linear theory. However, the main differences, viz., the broad experimental spectrum at large plasma densities and the large gap between the beam and the plasma (the lower right-hand graph), as well as the presence of low-frequency radiation simultaneously with high-frequency radiation, remain and call for further investigation, both theoretical and experimental.

The following may be said regarding the reasons for failure of the theory in the high-frequency region. If we start out from a reflectivity in the region of a transition from a plasma waveguide to a metallic waveguide in the form (3.1), which does not depend on the frequency, we can assume that the theoretical spectrum of the accelerator in Fig. 11 should correspond to the experimental spectrum. Actually, Eq. (3.1) is inadequate, most seriously in that it underestimates the reflectivity from this transition region in the high-frequency part of the spectrum. This question, however, requires a special investigation. An additional investigation is needed to calculate the radiation spectrum with consideration of the finite thickness of the plasma layer. The approximation of an infinitely thin layer, which was used in the calculations in Fig. 11, is clearly unsuitable in the range of radiation frequencies that are comparable to the plasma frequency. This can account for the discrepancy between theory and experiment at high frequencies (see Fig. 11, the case of $f_p=56$ GHz and $R_p=0.8$ cm).

We shall say a few words regarding the discrepancy between theory and experiment in the low-frequency portion of the spectrum. Two reasons for it, which appear already in the linear theory, have already been pointed out above. The first is the possibility of the generation of low-frequency oscillations when modes with $l \neq 0$ are excited. This question was discussed above within the linear theory, and it is seen from Fig. 10 that they have fairly large gain coefficients and can make an appreciable contribution to the observed spectrum. These modes were not taken into account in the nonlinear spectra presented in Fig. 11. In addition, when the finite thickness of the plasma is taken into account, the excitation of symmetric volume plasma waves, which is most efficient at low frequencies, becomes possible.

Finally, we point out another possibility for the experimental appearance of low-frequency radiation due to nonlin-

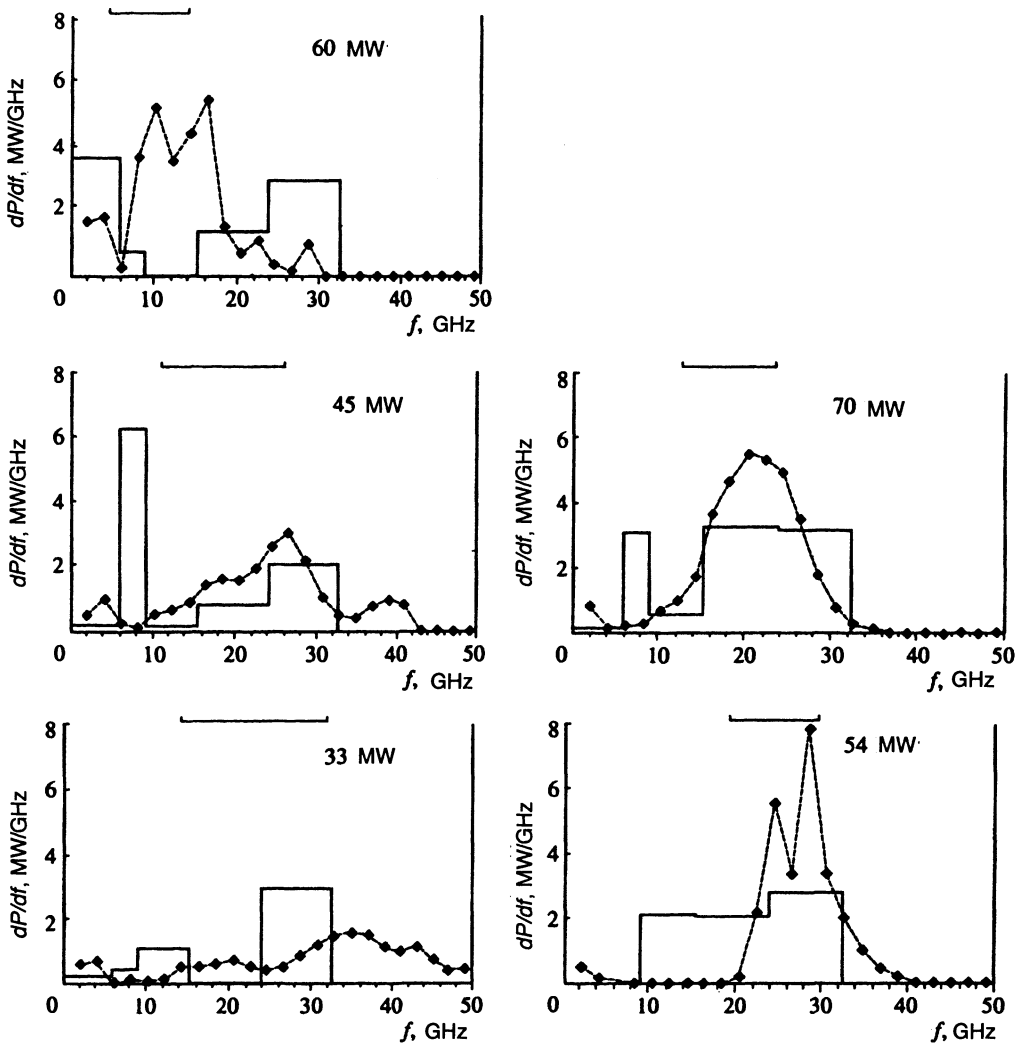

FIG. 11. Comparison of experimental and calculated spectra. The experimental spectra (solid lines) and the conditions under which they were recorded coincide completely in Fig. 9 and Fig. 5. The averaged radiated power for 30 shots is indicated on each graph. The calculated spectrum is plotted as a dotted line. The linear segment at the top of each graph shows the frequency range in which $\delta k > 0.5\delta k_{max}$ according to the linear theory.

ear phenomena. It can be exhibited, even if there is no mechanism for the linear excitation of modes with $l \neq 0$. Low frequencies can appear as a result of the decomposition of the $l=0$ mode into two modes with $l=\pm 1$. Such nonlinear decomposition is possible, if the so-called decomposition conditions are satisfied. This means that the doubled frequencies and the wave vector of the modes with $l=\pm 1$ fall in the band of frequencies and wave vectors $\omega(k_z)$ of the mode with $l=0$ excited by the relativistic electron beam. The experimentally observed range of low-frequency radiation does not contradict the decomposition conditions, since it falls in the region of the half-frequency of the high-frequency radiation. The quantitative resolution of this question requires additional theoretical and experimental investigations.

Thus, the spectrum of the complete radiation flux over the entire frequency range of a relativistic plasma microwave generator has been measured with an indication of the absolute values of the radiated energy in assigned frequency subranges. A radiated power equal to 85 MW, a radiation efficiency equal to 7%, a pulse duration equal to 18 ns, and a band of simultaneously generated frequencies extending over ~20 GHz have been recorded. The mean frequency of the radiation can be tuned from 19 to 27 GHz by varying the plasma density. The experimental results have been quantitatively compared with results calculated within the nonlinear theory. Partial agreement between theory and experiment has been discovered. The most important discrepancy is that the theoretically predicted narrowing of the spectrum as the gap between the hollow beam and the plasma increases and the plasma density increases was not observed experimentally. It would signify a transition from a Compton to a Raman generation mechanism. The progress which we have achieved in the diagnostics of microwave spectra and methods for numerical calculations can serve as a basis for solving this problem in the future.

This work was performed with the support of the Russian Foundation for Fundamental Research (Project No. 94-02-03437) and the International Science Foundation (Grants Nos. MO 3000 and MO 3300).

[1)]We shall refer mainly to reviews in which detailed bibliographies of the original investigations can be found.

[2)]This approximation is known in microwave electronics as the truncated equation (or slowly-varying-amplitude) method.

[1]A. I. Akhiezer and Ya. B. Faĭnberg, Dokl. Akad. Nauk SSSR **69**, 551 (1949).

[2]D. Bohm and E. P. Gross, Phys. Rev. **75**, 1851 (1949).

[3]G. A. Bernashevskiĭ, E. B. Bogdanov, and Z. S. Chernov, *Plasma and Electron Accelerators and Microwave Generators* [in Russian] (Sov. Radio, Moscow, 1965).

[4]R. J. Briggs, "Two-stream instabilities," in *Advances in Plasma Physics, Vol. 4*, edited by A. Simon and W. B. Thompson (Intersciences, New York, 1971), p. 43 [Russ. transl., Mir, Moscow, 1974, p. 131].

[5]D. I. Trubetskov and L. A. Pishchik, Fiz. Plazmy **15**, 342 (1989) [Sov. J. Plasma Phys. **15**, 200 (1989)].

[6]M. V. Kuzelev, F. Kh. Mukhametzyanov, M. S. Rabinovich *et al.*, Zh. Éksp. Teor. Fiz. **83**, 1358 (1982) [Sov. Phys. JETP **56**, 780 (1982)]; Dokl. Akad. Nauk SSSR **267**, 829 (1978) [Sov. Phys. Dokl. **27**, 1030 (1982)].

[7]M. V. Kuzelev and A. A. Rukhadze, Usp. Fiz. Nauk **152**, 285 (1987) [Sov. Phys. Usp. **30**, 507 (1987)].

[8]L. S. Bogdankevich, M. V. Kuzelev, and A. A. Rukhadze, Usp. Fiz. Nauk **133**, 3 (1981) [Sov. Phys. Usp. **24**, 1 (1981)].

[9]M. V. Kuzelev, A. A. Rukhadze, and D. S. Filippychev, in *Relativistic Microwave Electrons* [in Russian] (IPFAN, Gorkii, 1981), p. 170.

[10]M. V. Kuzelev and A. A. Rukhadze, in *Problems in Physics and Astrophysics (V. L. Ginzburg's 70th Birthday)* [in Russian] (Nauka, Moscow, 1989), p. 70.

[11]M. V. Kuzelev and A. A. Rukhadze, *Electrodynamics of Dense Electron Beams in a Plasma* [in Russian] (Nauka, Moscow, 1990), p. 331.

[12]M. V. Kuzelev, F. Kh. Mukhametzyanov, M. S. Rabinovich *et al.*, in *Relativistic Microwave Electrons* [in Russian] (IPFAN, Gorkii, 1981), p. 160.

[13]M. V. Kuzelev, A. A. Rukhadze, P. S. Strelkov, and A. G. Shkvarunets, Fiz. Plazmy **13**, 1370 (1987) [Sov. J. Plasma Phys. **13**, 793 (1987)].

[14]A. G. Shkvarunets, A. A. Rukhadze, and P. S. Strelkov, Fiz. Plazmy **20**, 682 (1994) [Plasma Phys. Rep. **20**, 613 (1994)].

[15]O. T. Loza, P. S. Strelkov, and A. G. Shkvarunets, Tr. Inst. Obshch. Fiz., Akad. Nauk **45**, 3 (1994).

[16]I. A. Selivanov, P. S. Strelkov, A. V. Fedotov, and A. G. Shkvarunets, Fiz. Plazmy **15**, 1283 (1989) [Sov. J. Plasma Phys. **15**, 744 (1989)].

Translated by P. Shelnitz